

The ringing of quantum corrected Schwarzschild black hole with GUP*

Yujia Xing¹, Yi Yang¹, Dong Liu¹, Zheng-Wen Long^{1†} and Zhaoyi Xu^{1‡}

¹College of Physics, Guizhou University, Guiyang, 550025, China

August 10, 2022

Abstract

Schwarzschild black holes with quantum corrections are studied under scalar field perturbations and electromagnetic field perturbations to analyze the effect of the correction term on the potential function and quasinormal mode (QNM). In classical general relativity, spacetime is continuous and there is no existence of the so-called minimal length. The introduction of the correction items of the generalized uncertainty principle (GUP), the parameter β , can change the singularity structure of the black hole gauge and may lead to discretization in time and space. We apply the sixth-order WKB method to approximate the QNM of Schwarzschild black holes with quantum corrections and perform numerical analysis to derive the results of the method. Also, we find that the effective potential and QNM in scalar fields are larger than those in electromagnetic fields.

Keywords: Quantum corrections, Black hole, Quasinormal mode, Generalized uncertainty principle

PACS: 04.70.Dy, 04.70.-s, 04.30.-w, 04.70.Bw

1. Introduction

Black holes are one of the most important predictions of Einstein's general theory of relativity, and in order to more fully understand the physical properties of black holes, physicists have constructed different black hole solutions [1,2]. The shadow of the M87 [3–5] massive black hole, surrounded by a crescent-shaped aperture, was first obtained by the Event Horizon Telescope. Therefore, the black hole at the heart of the M87 elliptical galaxy has also become a key object of observation and analysis for many physicists. The LIGO-VIRGO collaboration [6–9] has successfully detected gravitational waves from the combination of a black hole and a neutron star, and this discovery is extremely important for the study of black holes, in other words through the observation of gravitational waves we can fully understand the nature of the event horizon of black holes. Gravitational waves from some dense objects produce echoes [10–20] during propagation, which makes the echoes inseparably linked to the unique properties of dense objects, and one uses this signal to analyze the inherent properties of dense objects. It is also possible to observe gravitational wave echoes through the later stages of the QNM ringing.

Chandrasekhar [24] made a prominent contribution to the QNM in black holes, especially the effect of the

*Project supported by the National Natural Science Foundation of China (Grant Nos. 11465006, Grant Nos.11565009) and the Special Research Fund for Natural Science of Guizhou University (Grant No. X2020068).

†Corresponding author. E-mail:zwlong@gzu.edu.cn

‡Corresponding author. E-mail:zyxu@gzu.edu.cn

QNM on the external perturbation of the black hole, the essence of which is that there is a QNM ringing at the late stage of the initial pulse for the outside of the black hole event horizon. QNM [25–37] is the vibrational frequency that is available at the pure outgoing wave at infinity and the pure incident wave in the event horizon with free vibration. QNM has been widely applied in recent years, including QNM in dark matter halos [38–40], QNM in charged black holes with electromagnetic field perturbations [41], QNM in the multi-dimensional Einstein-power-Maxwell case with scalar field perturbations in the spacetime context of black holes [42], perturbation studies of black holes to solve spectral related problems [43], the relationship between QNM and shading with quantum correcting [44], calculation of slow revolving black holes with dynamical Chern-Simons gravity using QNM [21], and the accurate solutions of Kerr black hole perturbations by using QNM [22,23].

The solution of a black hole has a singularity, there is a singularity that would cause general relativity to fail at that point. Therefore, physicists have made a lot of research to conclude that the GUP can be used to correct the black hole degree gauge [45–49], and have achieved important results. In 1968, Bardeen presented the regular black hole solutions [50]. In [51], Kazakov and Solodukhin used quantum correction terms to deform the Schwarzschild solution to avoid singularities. The QNM of the corrected Schwarzschild solution has been analyzed in [52]. In [53], electrons can be emitted across the potential barrier into the vacuum and thus quantum corrected Schwarzschild black holes embodying Hawking radiation. In view of the importance of the QNM to reflect the relevant properties near the apparent horizon of the black hole event, we will study the QNM of the black hole with GUP correction considered in this paper.

This paper is structured as follows. In Sec.2, we use the equations of the quantum-corrected metric in the presence of scalar and electromagnetic field perturbations to derive the corresponding effective potential bases and draw an image of the effective potential. In Sec.3, numerical calculation by WKB method to obtain the frequency of QNM. In Sec.4, the conclusions of this study were drawn.

2. The methods

2.1. Scalar and electromagnetic field perturbations in quantum-corrected Schwarzschild black hole

The uncertainty principle of black holes suggests a relationship by which the uncertainty principle at the microscopic scale is linked to black holes at the macroscopic scale. This correspondence suggests the possible existence of black holes with masses below the Planck scale, but with order radius below the Compton scale rather than the Schwarzschild scale. To eliminate the singularity of the black hole metric, we use GUP to quantum correct the Schwarzschild black hole to analyze the QNM, as the Schwarzschild radius r_h is transformed into the GUP radius r_H [54], considering the GUP

$$\Delta x > \frac{h}{\Delta p} + \left(\frac{\alpha l_{\text{P}}^2}{\hbar}\right)\Delta p, \quad (1)$$

where α is positive dimensionless parameter, l_{P1} is the Planck length, $l_{\text{P1}} = \sqrt{\frac{\hbar G}{c^3}}$, M_{P1} is Planck mass, $M_{\text{P1}} = \sqrt{\frac{\hbar c}{G}}$, M_{C} is Compton mass, and considering $\Delta x \rightarrow R$, $\Delta p \rightarrow cM$, then becomes

$$R > R'_{\text{C}} \equiv \frac{\hbar}{M_{\text{C}}} + \frac{\alpha GM}{c^2} = \frac{\hbar}{M_{\text{C}}} \left[1 + \alpha \left(\frac{M}{M_{\text{P1}}} \right)^2 \right]. \quad (2)$$

GUP affects the size of the black hole horizon, then Eq.(2) is written as

$$R > R'_{\text{S}} = \frac{\alpha GM}{c^2} \left[1 + \frac{1}{\alpha} \left(\frac{M_{\text{P1}}}{M} \right)^2 \right]. \quad (3)$$

The free constant of Eq.(2) is related to the first term, then Eq.(2) and (3) are written as

$$R'_{\text{C}} = \frac{\beta \hbar}{M_{\text{C}}} \left[1 + \frac{2}{\beta} \left(\frac{M}{M_{\text{P1}}} \right)^2 \right] \quad (4)$$

and

$$R'_{\text{S}} = \frac{2GM}{c^2} \left[1 + \frac{\beta}{2} \left(\frac{M_{\text{P1}}}{M} \right)^2 \right] \quad (5)$$

where β is positive dimensionless parameter, $\hbar = c = G = 1$.

The corrected Schwarzschild black hole:

$$ds^2 = f(r)dt^2 - \frac{1}{f(r)}dr^2 - r^2(d\theta^2 + \sin^2\theta d\phi^2), \quad (6)$$

where

$$f(r) = 1 - \frac{2}{M_{\text{P1}}^2} \frac{M}{r} \left(1 + \frac{\beta}{2} \frac{M_{\text{P1}}^2}{M^2} \right), \quad (7)$$

and r_{H} is written as

$$r_{\text{H}} = \frac{2}{M_{\text{P1}}^2} \left(\frac{M^2 + \frac{\beta}{2} M_{\text{P1}}^2}{M} \right) = R'_{\text{S}}, \quad (8)$$

with Schwarzschild black hole horizon $r_{\text{h}}=2M$.

In this study, we focus on the analysis of spacetime in the context of Schwarzschild black holes after quantum corrections in scalar and electromagnetic fields. Then the radial equation and the effective potential are derived.

For the massless scalar field :

$$\frac{1}{\sqrt{-g}} \partial_{\mu} (\sqrt{-g} g^{\mu\nu} \partial_{\nu} \Phi) = 0. \quad (9)$$

For the electromagnetic field equation :

$$\frac{1}{\sqrt{-g}} \partial_{\nu} (F_{\rho\sigma} g^{\rho\mu} g^{\sigma\nu} \sqrt{-g}) = 0, \quad (10)$$

where $F_{\rho\sigma} = \partial_{\rho} A_{\sigma} - \partial_{\sigma} A_{\rho}$, A_{ν} is an electromagnetic four-potential.

The tortoise coordinate is expressed as:

$$dr_* = \frac{dr}{f(r)}. \quad (11)$$

By splitting the variances Eqs.(9) and (10), the equation typically takes the Schrodinger form:

$$-\frac{d^2\Psi}{dr_*^2} + V(r)\Psi = \omega^2\Psi. \quad (12)$$

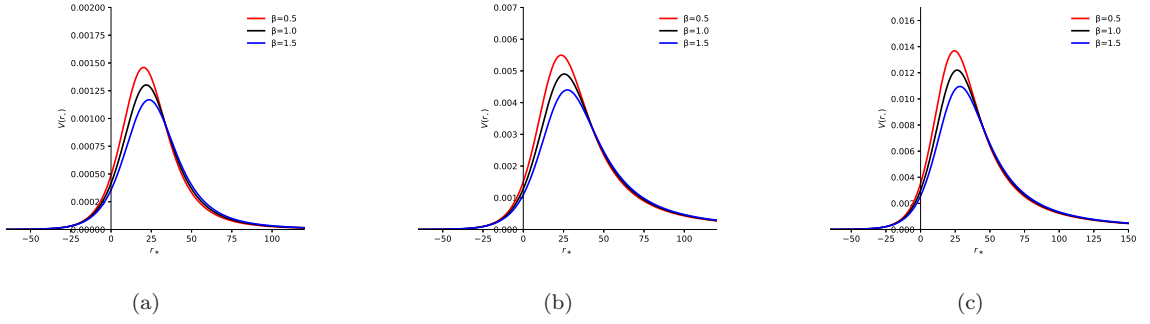


Figure 1: The effective potentials of the scalar field with the different l . (a) $l = 0$ (b) $l = 1$ (c) $l = 2$.

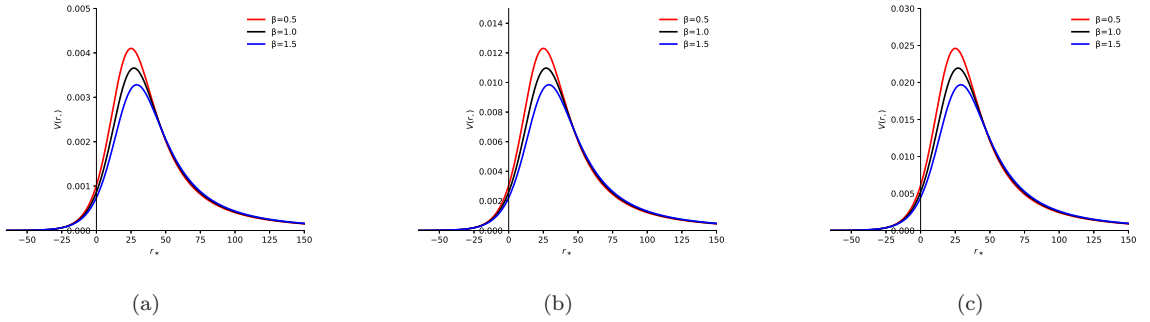


Figure 2: The effective potentials of the electromagnetic field with the different l . (a) $l = 1$ (b) $l = 2$ (c) $l = 3$.

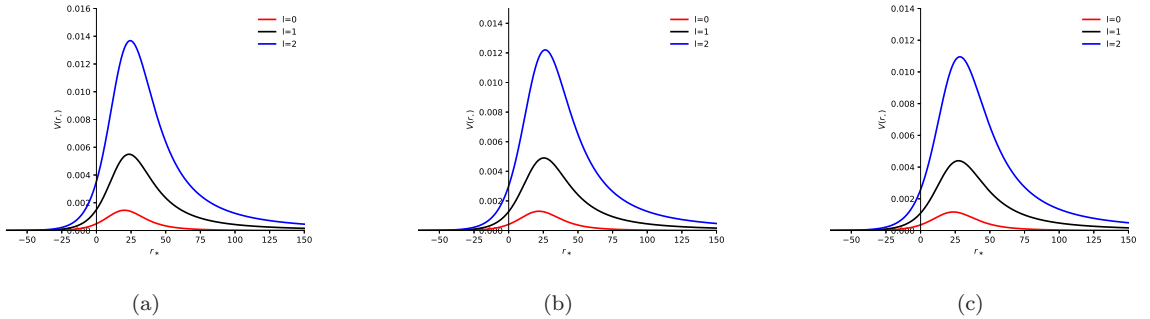


Figure 3: The effective potentials of the scalar field with the different β . (a) $\beta = 0.5$ (b) $\beta = 1.0$ (c) $\beta = 1.5$.

The effective potentials under the scalar and electromagnetic fields :

$$V_{\text{eff}} = \frac{f(r)}{r} \frac{df(r)}{dr} + \frac{f(r)l(l+1)}{r^2}, \quad (13)$$

$$V_{\text{em}} = \frac{f(r)l(l+1)}{r^2}. \quad (14)$$

Figs.1-4 show the effective potential for various parameters l and β . Figs.1-2 show that under the scalar and electromagnetic fields, when l is constant, the effective potential decreases with the increase of β , decays at infinity, and finally disappears, and then the black hole will return to the equilibrium state. Figs.3-4 show that when β is constant, the effective potential increases as l increases, and when r_* tends to infinity the effective potential approaches 0. Figs.5 show that when the parameters l and β are fixed, the effective potential of the

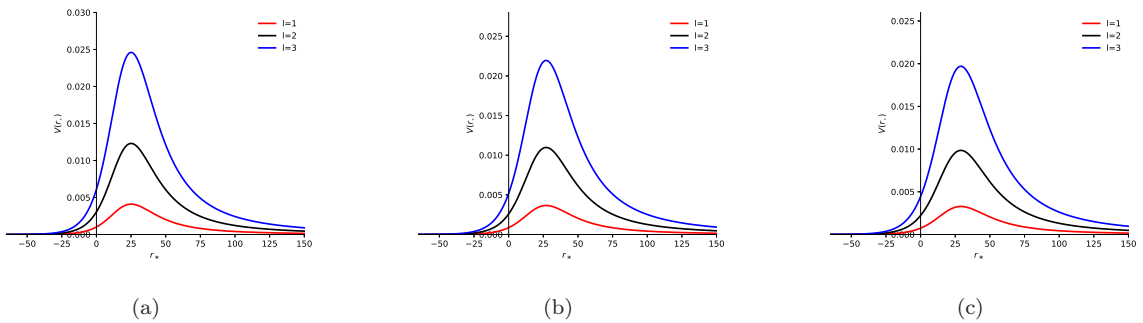


Figure 4: The effective potentials of the electromagnetic field with the different β . (a) $\beta = 0.5$ (b) $\beta = 1.0$ (c) $\beta = 1.5$.

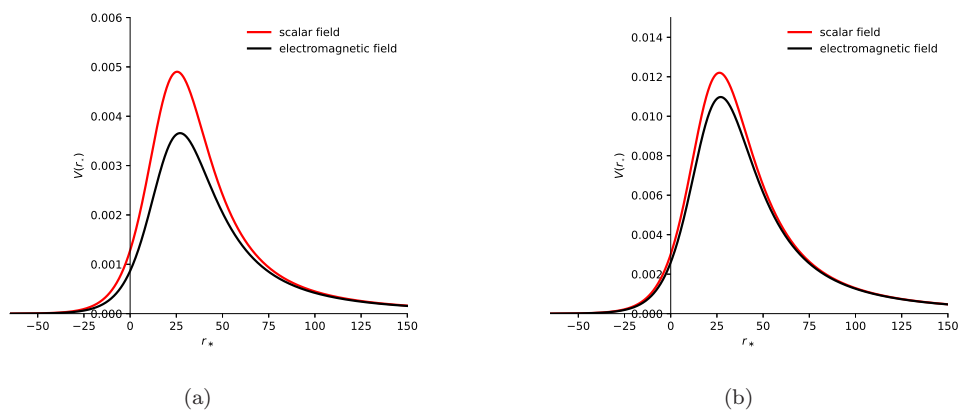


Figure 5: The effective potentials of the scalar and electromagnetic field. (a) $\beta = 1, l = 1$ (b) $\beta = 1, l = 2$.

scalar field is more than the effective potential of the electromagnetic field. In [55,56], the QNM and effective potential of black holes in Einstein-Ethernet theory and bumblebee gravity are studied with great research significance, where the effective potential increases with l . The effective potential of the scalar field is larger than the electromagnetic field when l is the same, and our conclusions are consistent with the results of this study.

2.2. The WKB method

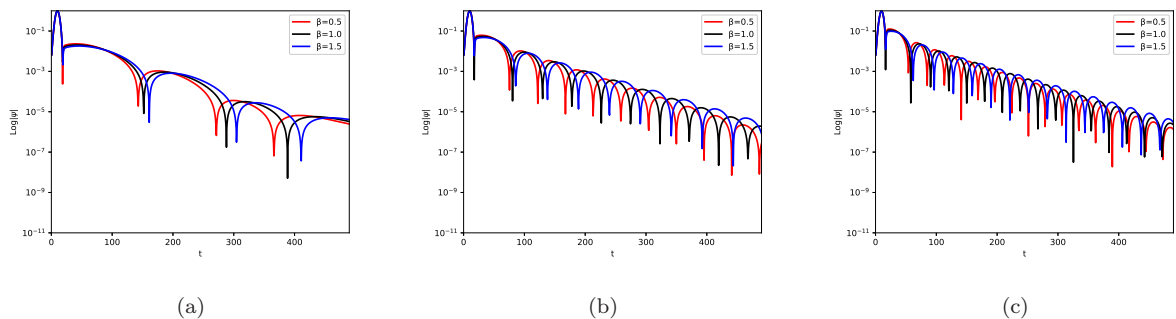
The WKB method was firstly introduced by Schutz and Will [25] and then further explained by Konoplya [26–28]. We use the WKB method to study frequencies, the main idea of which is to expand the WKB series in the asymptotic region and to match the solution of this expanding at infinity with the Taylor unfolding around the effective potential peak. In this session, we study the QNM frequencies by means of the sixth-order WKB formula of the shape given below:

$$\frac{i(\omega^2 - V_0)}{\sqrt{-2V_0''}} - \sum_{i=2}^6 \Omega_i = n + \frac{1}{2}, \quad (15)$$

where V_0 is the maximal value of the effective potential at r_0 , V_0'' is the second order of the derivatives of the tortoise coordinates, Ω_i are the correction terms.

Table 1: The QNM frequencies of scalar field.

WKB method				
β	$l = 0$	$l = 1$	$l = 2$	$l = 3$
0.25	0.026779 - 0.024441i	0.071008 - 0.023699i	0.117247 - 0.023458i	0.163725 - 0.023394i
0.50	0.025991 - 0.023722i	0.068919 - 0.023002i	0.113798 - 0.022768i	0.158910 - 0.022706i
0.75	0.025248 - 0.023044i	0.066950 - 0.022345i	0.110547 - 0.022118i	0.154369 - 0.022057i
1.00	0.024547 - 0.022404i	0.065091 - 0.021724i	0.107476 - 0.021503i	0.150081 - 0.021444i
1.25	0.023885 - 0.021797i	0.063331 - 0.021130i	0.104571 - 0.020922i	0.146025 - 0.020865i
1.50	0.023255 - 0.021224i	0.061665 - 0.020581i	0.101819 - 0.020371i	0.142182 - 0.020315i


 Figure 6: The dynamical evolutions of the scalar field with the different l . (a) $l = 0$ (b) $l = 1$ (c) $l = 2$.

2.3. The time domain method

The time-domain integration method proposed by Gundlach, Price and Pullin [57,58] to study the process of change of dynamical equations. We use this method to calculate the variation of frequency with time in the background spacetime of the black hole. By introducing the light cone coordinates for numerical computation

$$\begin{aligned} u &= t - r_*, \\ v &= t + r_*, \end{aligned} \quad (16)$$

where u and v are integration constants, r_* is tortoise coordinate. The wave function equation is being given as

$$-4 \frac{\partial^2 \psi(\mu, \nu)}{\partial \mu \partial \nu} = V(\mu, \nu) \psi(\mu, \nu). \quad (17)$$

The effective potential is influenced by the light cone variable (16). The difference step of the discretization is shown in [58], this discretization scheme is given by

$$\Psi(N) = \Psi(W) + \Psi(E) - \Psi(S) - h^2 \frac{V(W)\Psi(W) + V(E)\Psi(E)}{8} + O(h^4). \quad (18)$$

Where we use the following specified points $N = (u+h, v+h)$, $W = (u+h, v)$, $E = (u, v+h)$ and $S = (u, v)$, where $\nu = \nu_0$, $\mu = \mu_0$ are the initial datas. In order to contain the accuracy of the frequency analysis, we can control the parameters of the mathematical combination, adjust the differential grid and accuracy [59].

Table 2: The QNM frequencies of electromagnetic field.

WKB method				
β	$l = 1$	$l = 2$	$l = 3$	$l = 4$
0.25	0.0601676 - 0.022457i	0.110932 - 0.023033i	0.159248 - 0.023179i	0.206811 - 0.023238i
0.50	0.058398 - 0.021796i	0.107669 - 0.022355i	0.154564 - 0.022498i	0.200728 - 0.022555i
0.75	0.0567295 - 0.021174i	0.104593 - 0.021716i	0.150148 - 0.021855i	0.194993 - 0.021910i
1.00	0.055153 - 0.020586i	0.101687 - 0.021113i	0.145977 - 0.021248i	0.189577 - 0.021302i
1.25	0.053663 - 0.020029i	0.098939 - 0.020541i	0.142032 - 0.020674i	0.184453 - 0.020726i
1.50	0.052250 - 0.019502i	0.096335 - 0.020002i	0.138294 - 0.020129i	0.179599 - 0.020181i

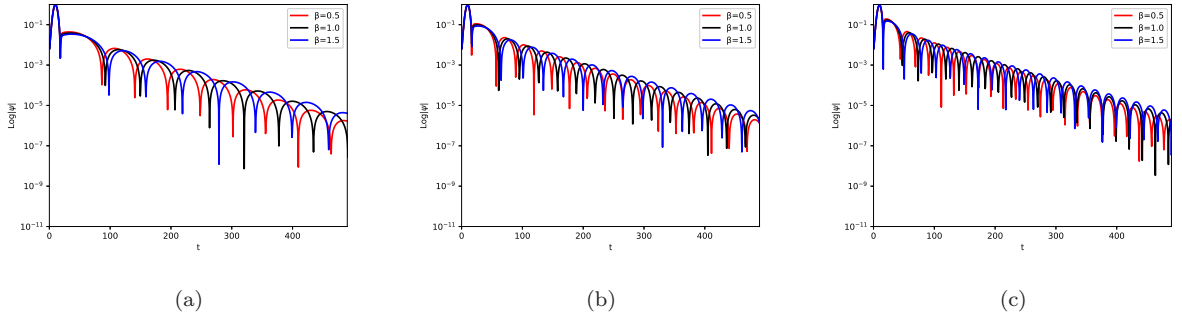


Figure 7: The dynamical evolutions of the electromagnetic field with the different l . (a) $l = 1$ (b) $l = 2$ (c) $l = 3$.

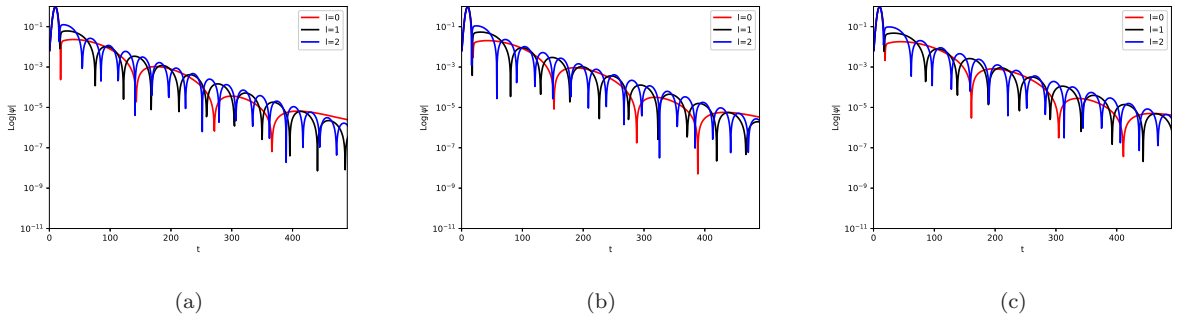


Figure 8: The dynamical evolutions of the scalar field with the different β . (a) $\beta = 0.5$ (b) $\beta = 1.0$ (c) $\beta = 1.5$.

3. Quantum-corrected Schwarzschild black hole model

In this section, we discuss the variation law of QNM for scalar and electromagnetic fields. To obtain the law we analyze the GUP corrected Schwarzschild black hole degree gauge, where the solution to Eq.(17) reflects the evolution process of the QNM. We respectively take $M = 1$, $M_{P1} = 0.5$, the different parameters of l and β , and then find the QNM variation law. We know that the variation law of the QNM for the modified Schwarzschild black hole is related to the effective potential. Since we want to quantitatively analyze this qualitative action, we have worked out the QNM frequencies via the sixth-order WKB method in the presence of scalar and electromagnetic fields. According to Tables 1-2, it can be seen that the corrected Schwarzschild black hole

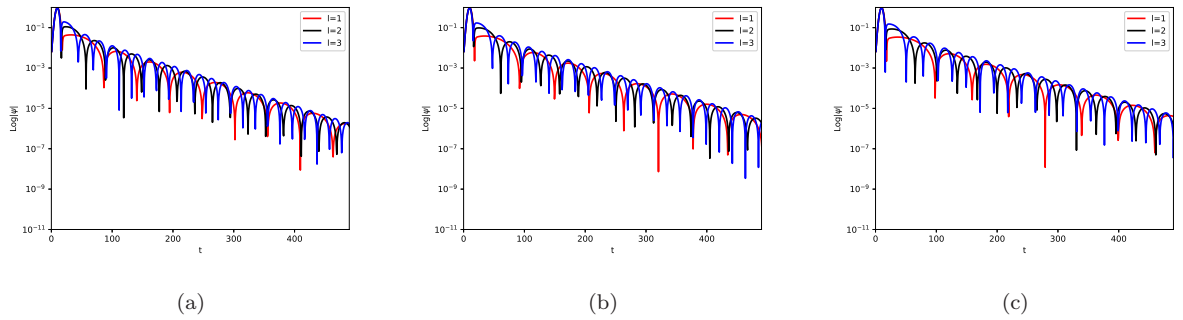


Figure 9: The dynamical evolutions of the electromagnetic field with the different β . (a) $\beta = 0.5$ (b) $\beta = 1.0$ (c) $\beta = 1.5$.

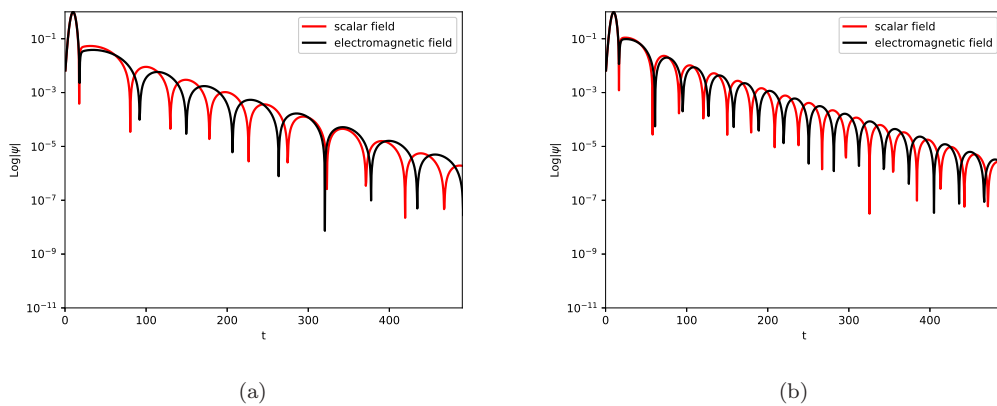


Figure 10: The dynamical evolutions of the scalar and electromagnetic field. (a) $\beta = 1, l = 1$ (b) $\beta = 1, l = 2$.

returns to steady state after a period of perturbation because the real part of the frequency is positive and the imaginary part is negative. As l is the same, the real imaginary parts of QNMs are decreasing as β increases, in other words, the oscillation frequency and damping rate are decreasing, and the more β the slower the decay. Our results are opposite to the variation pattern of the real and imaginary parts of the QNM of the second kind aether black hole in [55], whose real and imaginary parts of the QNM decrease with decreasing parameters c_{13} . In the scalar field, when β is the same, as l increases, the real part of QNM increases and the imaginary part decreases. With larger l , the real part grows more rapidly and the imaginary part decays more slowly. In the electromagnetic field, the real and imaginary parts of the QNM increase as l increases. In a physical sense, the introduction of the parameter β can transform the singularity construction of the black hole metric since there are singularities in the solution of the black hole. This new GUP of correction items may contribute to the discretization in time and space.

As can be seen from Figs.6-7, for l to be a constant value, the period of the QNM perturbation time is the shortest when $\beta = 0.5$, followed by $\beta = 1.0$ and the longest period of the QNM perturbation when $\beta = 1.5$. In Figs.8, it can be seen that when β is a fixed value, the period of the perturbation time of QNM is the least when l is much larger, and the magnitude of its period time is $l = 0 > l = 1 > l = 2$. Our results are in agreement with the conclusion of the time-domain diagram of the QNM for black holes in bumblebee gravity [56] under the scalar field that the parameter l affects the oscillation of the QNM, and the larger l is,

the easier the QNM is to detect. Similarly, in Figs.9, the magnitude of the cycle time of the perturbation time of QNM is $l = 1 > l = 2 > l = 3$. Figs.10 show that if the parameters l and β are fixed, the QNM of the scalar field is greater than the effective potential of the electromagnetic field. The average value of the ringing of the QNM in the scalar and electromagnetic fields is about 10^{-1} and 10^{-8} . We can observe that the perturbation process in Fig.6(a) is clearly different from Fig.6(b) and Fig.6(c), due to the fact that the parameter l affects the frequency of the QNM.

4. Conclusions

In the present work, we study the QNM of the Schwarzschild black hole corrected by the GUP. We analyze the equations in scalar and electromagnetic fields and obtain the effective potential which corresponds to them. The calculation is performed by the sixth-order WKB method, which gives the frequency of the QNM. We mainly obtained the following results:

(1)The effective potential of the GUP quantum-corrected Schwarzschild black hole decrease with the increase of β , and increase with the increase of l . When r_* approaches infinity, the effective potential tends to 0 and the black hole will be unaffected by the change of parameters and finally comes back to the equilibrium state.

(2)The QNM ringing of the GUP quantum-corrected Schwarzschild black hole appears after the initial pulse. When l is fixed, the QNM oscillation becomes weaker as β increases, the correction term of GUP makes the black hole metric gauge not singular; when β is fixed, the QNM oscillation becomes stronger as l increases. It can be concluded that the trend of QNM is related to the effective potential.

(3)The QNM is a special characteristic of the solution of the black hole perturbation equation, which occupies the main time in the black hole perturbation process. The parameter l influences the perturbation time of QNM, among the most obvious in Fig.6(a), which affects the spacetime with black hole background. In other words, it affects the intrinsic frequency as well as the damping rate of the oscillation and is not affected by the initial oscillation.

(4)In Figs.6-7, when l is a constant value, the period of the time of QNM perturbation is $\beta = 1.5 > \beta = 1.0 > \beta = 0.5$, then $\beta = 0.5$ is easier to detect. In Fig.8, it is known that whenever β is a constant value, the duration of the perturbation time is $l = 0 > l = 1 > l = 2$, then $l = 2$ is more easily to be detected. In Fig.9, it is well recognized that as long as β is a constant, the length of the perturbation time is $l = 1 > l = 2 > l = 3$, then $l = 3$ is easy to be found.

(5)The average value of the ringing of QNM in scalar and electromagnetic fields is about in the range of 10^{-1} and 10^{-8} , which is in agreement with our results in Tables 1-2 .

(6)The QNM ringing of the scalar is larger than that of the electromagneticfield field, which means that the radiation excited by the perturbation in the scalar field may be larger than that excited by the electromagneticfield field.

In the present work, we have taken into account the scalar and electromagnetic field perturbations, and it is known that the QNM signals of both perturbations have very close physical effects in the vicinity of the black hole horizon. It is of significance that the gravitational field perturbation is also very interesting, and according to the study [60–63], the QNM signal can also be produced under gravitational perturbation. More gravitational radiation is produced under the gravitational field than under the outfield perturbation. Similarly

we think it is also an interesting topic to consider quantum corrections below Schwarzschild black holes under gravitational fields.

References

- [1] Arias P J, Barge P, Contreras E and Fuenmayor E 2022 2+1 Einstein-Klein-Gordon black holes by gravitational decoupling *Astronomy* **1** 2-14
- [2] Dymnikova I , Dobosz A and So Błtysek 2022 Classification of Circular Equatorial Orbits around Regular Rotating Black Holes and Solitons with the de Sitter/ Phantom Interiors *Universe* **8** 2 65
- [3] Akiyama K *et al.* [Event Horizon Telescope] 2019 First M87 Event Horizon Telescope Results. I. The Shadow of the Supermassive Black Hole *Astrophys. J. Lett.* **875** 1 L1
- [4] Akiyama K *et al.* [Event Horizon Telescope] 2019 First M87 Event Horizon Telescope Results. II. Array and Instrumentation *Astrophys. J. Lett.* **875** 1 L2
- [5] Akiyama K *et al.* [Event Horizon Telescope] 2019 First M87 Event Horizon Telescope Results. III. Data Processing and Calibration *Astrophys. J. Lett.* **875** 1 L3
- [6] Abbott B P *et al.* [LIGO Scientific and Virgo] 2016 Astrophysical Implications of the Binary Black-Hole Merger GW150914 *Astrophys. J. Lett.* **818** 2 L22
- [7] Abbott B P *et al.* [LIGO Scientific and Virgo] 2016 Observation of Gravitational Waves from a Binary Black Hole Merger *Phys. Rev. Lett.* **116** 6 061102
- [8] Abbott B P *et al.* [LIGO Scientific and Virgo] 2016 Binary Black Hole Mergers in the first Advanced LIGO Observing Run *Phys. Rev. X* **6** 4 041015
- [9] Abbott B P *et al.* [LIGO Scientific and VIRGO] 2017 GW170104: Observation of a 50-Solar-Mass Binary Black Hole Coalescence at Redshift 0.2 *Phys. Rev. Lett.* **118** 22 221101
- [10] Yang Y, Liu D , Xu Z, Xing Y, Wu S and Long Z W 2021 Echoes of novel black-bounce spacetimes *Phys. Rev. D* **104** 10 104021
- [11] Churilova M S and Stuchlik Z 2020 Ringing of the regular black-hole/wormhole transition *Class. Quant. Grav.* **37** 7 075014
- [12] Bronnikov K A and Konoplya R A 2020 Echoes in brane worlds: ringing at a black hole–wormhole transition *Phys. Rev. D* **101** 6 064004
- [13] Wang Y T, Li Z P , Zhang J, Zhou S Y and Piao Y S 2018 Are gravitational wave ringdown echoes always equal-interval? *Eur. Phys. J. C* **78** 482
- [14] Testa A and Pani P 2018 Analytical template for gravitational-wave echoes: signal characterization and prospects of detection with current and future interferometers *Phys. Rev. D* **98** 044018
- [15] Cardoso V and Pani P 2017 Tests for the existence of black holes through gravitational wave echoes *Nature Astron* **1** 586
- [16] Konoplya R A, Stuchl Z ík and Zhidenko A 2019 Echoes of compact objects: new physics near the surface and matter at a distance *Phys. Rev. D* **99** 024007
- [17] Ezquiaga J M, Hu W, Lagos M and Lin M X 2021 Gravitational wave propagation beyond general relativity: waveform distortions and echoes *JCAP* **11** 11 048
- [18] Cardoso V, Foit V F and Kleban M 2019 Gravitational wave echoes from black hole area quantization *JCAP* **08** 006
- [19] Chesler P M, Blackburn L, Doeleman S S, Johnson M D, Moran J M, Narayan R and Wielgus M 2021 Light echos and coherent autocorrelations in a black hole spacetime *Class. Quant. Grav.* **38** 12 125006
- [20] Cadonati L 2010 Laser Interferometers, Gravitational waves and Echos from the Universe *J. Phys. Conf. Ser.* **222** 012030
- [21] Srivastava M, Chen Y and Shankaranarayanan S 2021 Analytical computation of quasinormal modes of slowly rotating black holes in dynamical Chern-Simons gravity *Phys. Rev. D* **104**, 6, 064034
- [22] Bonelli G, Iossa C, Lichtig D P and Tanzini A 2022 Exact solution of Kerr black hole perturbations via CFT2 and instanton counting: Greybody factor, quasinormal modes, and Love numbers *Phys. Rev. D* **105** 4 044047
- [23] Carullo G, Laghi D, Johnson-McDaniel N K, Del Pozzo W, Dias O J C, Godazgar M and Santos J E 2022 Constraints on Kerr-Newman black holes from merger-ringdown gravitational-wave observations *Phys. Rev. D* **105** 6 062009
- [24] Chandrasekhar S 1983 *The Mathematical Theory of Black Holes* (Oxford: Clarendon)

- [25] Schutz B F and Will C M 1985 BLACK HOLE NORMAL MODES: A SEMIANALYTIC APPROACH *Astrophys. J. Lett.* **291** L33-L36
- [26] Iyer S and Will C M 1987 Black Hole Normal Modes: A WKB Approach. 1. Foundations and Application of a Higher Order WKB Analysis of Potential Barrier Scattering *Phys. Rev. D* **35** 3621
- [27] Iyer S 1987 BLACK HOLE NORMAL MODES: A WKB APPROACH. 2. SCHWARZSCHILD BLACK HOLES *Phys. Rev. D* **35** 3632
- [28] Konoplya R A 2003 Quasinormal behavior of the d-dimensional Schwarzschild black hole and higher order WKB approach *Phys. Rev. D* **68** 024018
- [29] Bezares M, Bošković M, Liebling S. , Palenzuela C, Pani P and Barausse E 2022 Gravitational waves and kicks from the merger of unequal mass, highly compact boson stars *Phys. Rev. D* **105** 6 064067
- [30] Vieira H S, Destounis K and Kokkotas K D 2022 Slowly-rotating curved acoustic black holes: Quasinormal modes, Hawking-Unruh radiation, and quasibound states *Phys. Rev. D* **105** 4 045015
- [31] Fernandes T V, Hilditch D, Lemos J P S and Cardoso V 2022 Quasinormal modes of Proca fields in a Schwarzschild-AdS spacetime *Phys. Rev. D* **105** 4 044017
- [32] Cano P A, Fransen K, Hertog T and Maenaut S 2022 Gravitational ringing of rotating black holes in higher-derivative gravity *Phys. Rev. D* **105** 2 024064
- [33] Cadoni M, Oi M and Sanna A P 2021 Quasinormal modes and microscopic structure of the Schwarzschild black hole *Phys. Rev. D* **104** 12, L121502
- [34] Mondkar S, Mukhopadhyay A, Rebhan A and Soloviev A 2021 Quasinormal modes of a semi-holographic black brane and thermalization *JHEP* **11**, 080
- [35] Destounis K, Macedo R P, Berti E, Cardoso V and Jaramillo J L 2021 Pseudospectrum of Reissner-Nordström black holes: Quasinormal mode instability and universality *Phys. Rev. D* **104** 8 084091
- [36] Srivastava M, Chen Y and Shankaranarayanan S 2021 Analytical computation of quasinormal modes of slowly rotating black holes in dynamical Chern-Simons gravity *Phys. Rev. D* **104** 6 064034
- [37] Cai X C and Miao Y G 2021 Quasinormal modes and shadows of a new family of Ayón-Beato-García black holes *Phys. Rev. D* **103** 12, 124050
- [38] Liu D, Yang Y, Wu S, Xing Y, Xu Z and Long Z W 2021 Ringing of a black hole in a dark matter halo *Phys. Rev. D* **104** 10 104042
- [39] Zhang C, Zhu T and Wang A 2021 Gravitational axial perturbations of Schwarzschild-like black holes in dark matter halos *Phys. Rev. D* **104** 12 124082
- [40] Barausse E, Cardoso V and Pani P 2014 Can environmental effects spoil precision gravitational-wave astrophysics? *Phys. Rev. D* **89** 10 104059
- [41] Nomura K and Yoshida D 2022 Quasinormal modes of charged black holes with corrections from nonlinear electrodynamics *Phys. Rev. D* **105** 4 044006
- [42] Liu Y and Jing J L 2012 Propagation and evolution of a scalar field in Einstein-Power-Maxwell spacetime *Chin. Phys. Lett.* **29** 010402
- [43] Hatsuda Y and Kimura M 2021 Spectral Problems for Quasinormal Modes of Black Holes *Universe* **7** 12 476
- [44] Okyay M and Övgün A 2022 Nonlinear electrodynamics effects on the black hole shadow, deflection angle, quasinormal modes and greybody factors *JCAP* **01** 01 009
- [45] Anacleto M A, Campos J A V , Brito F A and Passos E 2021 Quasinormal modes and shadow of a Schwarzschild black hole with GUP *Annals Phys.* **434** 168662
- [46] Anacleto M A, Brito F A, Luna G C and Passos E 2022 The generalized uncertainty principle effect in acoustic black holes *Annals Phys.* **440** 168837
- [47] Anacleto M A, Brito F A, Garcia C V, Luna G C and Passos E 2019 Quantum-corrected rotating acoustic black holes in Lorentz-violating background *Phys. Rev. D* **100** 10 105005
- [48] Sakalli I, Övgün A and Jusufi K 2016 GUP Assisted Hawking Radiation of Rotating Acoustic Black Holes *Astrophys. Space Sci.* **361** 10 330
- [49] Maluf R V and Neves J C S 2018 Thermodynamics of a class of regular black holes with a generalized uncertainty principle *Phys. Rev. D* **97** 10 104015

- [50] Bardeen J M 1968 Non-singular general relativistic gravitational collapse in Proc. Int. Conf. GR5 (Tbilisi, Georgia, USSR,) p. 174.
- [51] Kazakov D I and Solodukhin S N 1994 On Quantum deformation of the Schwarzschild solution *Nucl. Phys. B* **429** 153-176
- [52] Konoplya R A 2020 Quantum corrected black holes: quasinormal modes, scattering, shadows *Phys. Lett. B* **804** 135363
- [53] Hajebrahimi M and Nozari K 2020 A quantum-corrected approach to black hole radiation via a tunneling process *PTEP* **2020** 4 043E03
- [54] Carr B J, Mureika J and Nicolini P 2015 Sub-Planckian black holes and the Generalized Uncertainty Principle *JHEP* **07** 052
- [55] Ding C Quasinormal ringing of black holes in Einstein-aether theory 2017 *Phys. Rev. D* **96** 10 104021
- [56] Oliveira R, Dantas D M and Almeida C A S 2021 Quasinormal frequencies for a black hole in a bumblebee gravity *EPL* **135** 1 10003
- [57] Gundlach C., Price R H and Pullin J 1994 Late time behavior of stellar collapse and explosions: 1. Linearized perturbations *Phys. Rev. D* **49** 883-889
- [58] Gundlach C, Price R H and Pullin J 1994 Late time behavior of stellar collapse and explosions: 2. Nonlinear evolution *Phys. Rev. D* **49** 890-899
- [59] Moderski R and Rogatko M 2005 Evolution of a self-interacting scalar field in the spacetime of a higher dimensional black hole *Phys. Rev. D* **72** 044027
- [60] Dong R. and Stojkovic D 2021 Gravitational wave echoes from black holes in massive gravity *Phys. Rev. D* **103** 024058
- [61] Dey R, Chakraborty S and Afshordi N 2020 Echoes from braneworld black holes *Phys. Rev. D* **101** 104014
- [62] Dey R, Biswas S and Chakraborty S 2021 Ergoregion instability and echoes for braneworld black holes: Scalar, electromagnetic, and gravitational perturbations *Phys. Rev. D* **103** 084019
- [63] Oshita N, Tsuna D and Afshordi N 2020 Quantum Black Hole Seismology I: Echoes, Ergospheres, and Spectra *Phys. Rev. D* **102** 024045